

GLOBAL AND REGIONAL THERMOPHYSICAL PROPERTIES OF THE SURFACE OF ASTEROID RYUGU. Y. Shimaki¹, H. Senshu², N. Sakatani¹, T. Okada^{1,3}, T. Fukuhara⁴, S. Tanaka^{1,5}, M. Taguchi⁴, T. Arai⁶, H. Demura⁷, K. Suko⁷, T. Sekiguchi⁸, T. Kouyama⁹, J. Takita¹⁰, S. Hasegawa¹. ¹Institute of Space and Astronautical Science, Japan Aerospace Exploration Agency (3-1-1 Yoshinodai, Chuo, Sagamihara, Kanagawa 252-5210, Japan, shimaki@planeta.sci.isas.jaxa.jp). ²Chiba Institute of Technology, Japan. ³University of Tokyo, Japan. ⁴Rikkyo University, Japan. ⁵The Graduate University for Advanced Studies, SOKENDAI, Japan. ⁶Ashikaga University, Japan. ⁷University of Aizu, Japan. ⁸Hokkaido University of Education, Japan. ⁹National Institute of Advanced Industrial Science and Technology (AIST), Japan. ¹⁰Hokkaido Kitami Hokuto High School, Japan.

Introduction: The surface grain size of Ryugu was estimated to be 3 to 30 mm before the arrival of the Hayabusa2 [1], from the thermal inertia of 150 to 300 J m⁻² K⁻¹ s^{-0.5} (hereafter tiu) estimated by the ground observations [2] and a thermal conductivity model based on the laboratory experiments [3]. After the arrival, ONC revealed that the surface of Ryugu is covered by numerous boulders [4]. A close-up ONC image taken on October 15, 2018, showed that the size of boulders and particles on the surface of Ryugu is > several centimeters, which is thicker than the typical diurnal thermal skin depth of Ryugu [5]. TIR observations showed that the diurnal surface temperatures exhibit flat patterns, suggesting the effects of the surface roughness. Furthermore, the roughly estimated global thermal inertia of 300 ± 100 tiu [6] indicates the presence of porous materials on the surface. The thermal inertia of a single cauliflower-like dark boulder is estimated to be 280⁺⁹⁵-₃₈ tiu by MARA on MASCOT lander [7]. Since the thermophysical models (TPMs) have different implementations for the surface roughness, we examined the thermophysical properties of Ryugu by using different TPMs. Here we report the global and regional variations of the thermal inertia and surface roughness of Ryugu estimated by comparing the observation and calculation results.

Methods: We used the high-resolution thermal images for the one-rotation period acquired on August 1, 2018, taken from an altitude of 5 km, corresponding to ~4.5 m/pixel [6]. The raw thermal images were converted to the temperature images, then projected onto a shape model of Ryugu (SFM_200k_v20180804 [8]) to trace the diurnal temperatures of a surface of Ryugu. We assumed an emissivity of 0.9. The solar phase angle was ~20°, the sub-solar latitude was 8.4°S, and the heliocentric distance was 1.06 au. We omitted the first four and the last four temperatures in a diurnal temperature profile from the analyses since these temperatures acquired in the early morning and late evening that potentially represent various surface temperatures within a TIR pixel.

We used two TPMs: One is TPM1 based on [9] that utilizes the shape model of Ryugu and well reproduces large scale features such as self-heating at the roots of boulders. The other is TPM2 based on [10]

that utilizes shape models of rough fractal surface and well reproduces flat diurnal temperature profiles. We used the position configurations of the spacecraft, Ryugu, and the Sun on August 1, 2018, and assumed an emissivity of 0.9 for both calculations. We used albedo of 0.045 (bond albedo [11]) for TPM1 and 0.0146 (geometric albedo [4]) for TPM2. The parameters are the thermal inertia Γ from 20 to 800 tiu for TPM1, and Γ from 10 to 800 tiu, the surface roughness σ from 0 to 0.5, and the latitude θ from -88° to 88° for TPM2.

With TPM1, the thermal inertia of a facet on the shape model for Ryugu was estimated from the observed maximum temperature, so the pattern of the temperature profile was not considered. With TPM2, the thermal inertia and surface roughness of the facet is estimated by comparing the temperature profiles observed by TIR and those calculated by TPM2.

The temperature profiles by TPM2 with $|\theta| \leq 64^\circ$ are fitted by 4-order polynomial functions in the local time range from 8.6 to 16.6 hours to characterize the maximum temperature, its local time, and the curvature of the profile. To have dense reference datasets, the fitting coefficients of the function were interpolated in θ , σ , and Γ . Finally, we obtained 4,080 reference datasets with various (Γ , σ) for each latitude. For a facet of the shape model of Ryugu located at a latitude θ and a longitude φ , we used the effective latitude $\theta_{\text{eff}} = \theta + \theta_{\text{NS}}$ and the effective longitude $\varphi_{\text{eff}} = \varphi + \varphi_{\text{EW}}$ of the facet, where θ_{NS} and φ_{EW} are the tilt angles of the facet in North-to-South and East-to-West directions, respectively. The root means square (RMS) values between the observed and calculated temperatures in the local time range were calculated for each of the 4,080 reference datasets. We adopted the thermal inertia and roughness values at the minimum RMS value (Figure 1). We set the threshold RMS as 10 K.

Results and Discussions: The apparent surface temperatures of Ryugu showed low contrast except for the asteroid rim. The diurnal surface temperatures of Ryugu showed a more flat pattern than those of TPM1. The global thermal inertia with a standard deviation of Ryugu was estimated to be 278 ± 138 tiu by TPM1. The distribution of the thermal inertia, however, shows

a peak at the equatorial ridge, because of the neglect of the effect of the surface roughness on the apparent surface temperatures, thus we used the TPM2.

We confirmed that TPM2 successfully reproduced the observed temperature profiles at the southern hemisphere, although it is difficult to obtain $\text{RMS} < 10 \text{ K}$ at most of the northern hemisphere because of the observed non-smooth temperature profiles. The global thermal inertia of Ryugu estimated by TPM2 with $\text{RMS} < 10 \text{ K}$ is $225 \pm 45 \text{ tiu}$ (Figure 2), consistent with the ground observations [2] and the previous study [6]. We see slightly higher thermal inertia values ($\sim 350 \text{ tiu}$) at the northern slope of the equatorial ridge, where the temperature is lower than the surrounding terrains. We examined the thermal inertia of the interior of type I and II craters [12] with a diameter $> 100 \text{ m}$ and found these values are within the global average. The global surface roughness is estimated to be 0.41 ± 0.08 , corresponding to moderately high roughness. We confirmed that the high roughness value of 0.44 ± 0.07 in the Kibidango crater where the abundant boulders with a size of $> 1 \text{ m}$ are observed by ONC [4]. We found a low roughness region on the equatorial ridge (~ 0.3). This may be a result of the mass movement of regolith and boulders from the equatorial ridge to the mid-latitudes [13].

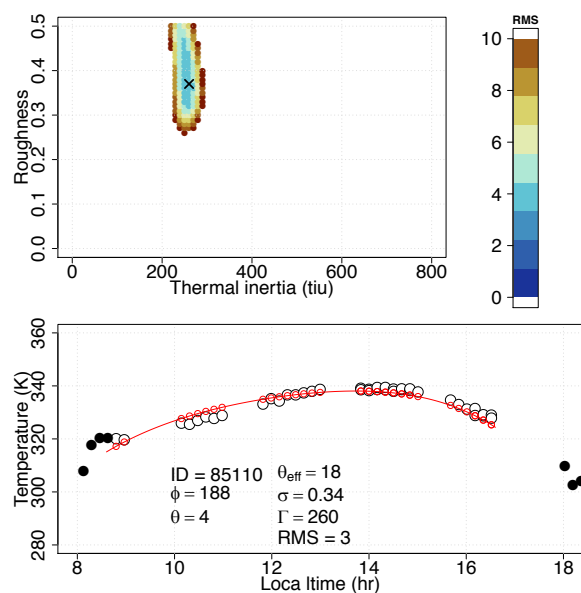


Figure 1. Estimation of the thermal inertia and surface roughness using TPM2. (top) The RMS color map, with the minimum RMS (cross), in the thermal inertia and roughness space for a facet of the shape model of Ryugu. (bottom) The observed temperature data used in the analysis (white circles) and omitted (black circles) with the estimated temperature profile (red circles with a curve).

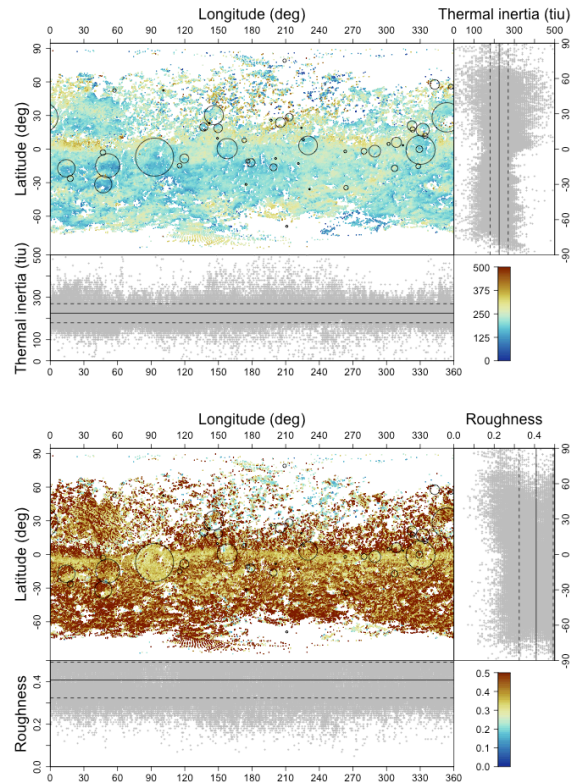


Figure 2. Thermophysical properties of the surface of Ryugu. (top) Thermal inertia estimated by TPM2 with $\text{RMS} < 10 \text{ K}$. Type I and II craters [13] are shown by circles. (bottom) Surface roughness estimated by TPM2 with $\text{RMS} < 10 \text{ K}$.

Acknowledgments: The authors would like to thank the Hayabusa2 team members for their technical and operational support and helpful scientific discussions. This study is supported by the JSPS Grants-in-Aid for Scientific Research (KAKENHI JP17H06459 and JP19H01951) and the JSPS Core-to-Core program “International Network of Planetary Sciences”.

References: [1] Wada, K. et al. (2018). *PEPS*, 5(1), 82. [2] Müller T.G. et al. (2017) *A&A*, 599:A103. [3] Sakatani, N. et al. (2017). *AIP Advances*, 7(1), 015310. [4] Sugita S. et al. (2019) *Science*, 364(6437), eaaw0422. [5] Sakatani, N. et al. (2019). *LPSC 50th*, #1732. [6] Okada, T. et al. (2020). *Nature*, in revision. [7] Grott M. et al. (2019) *Nature Astronomy*. doi: 10.1038/s41550-019-0832-x. [8] Watanabe S. et al. (2019) *Science*, 364(6437), 268–272. [9] Takita J. et al. (2017) *SSR*, 208(1- 4):287–315. [10] Senshu H. et al. (2017) *LPSC 48th*, #1950. [11] Ishiguro M. et al. (2014) *ApJ*, 792(1):74. [12] Hirata, N. et al. (2020). *Icarus*, 338, 113527. [13] Morota, T. et al. (2020). *Science*, in revision.